

LETTER • OPEN ACCESS

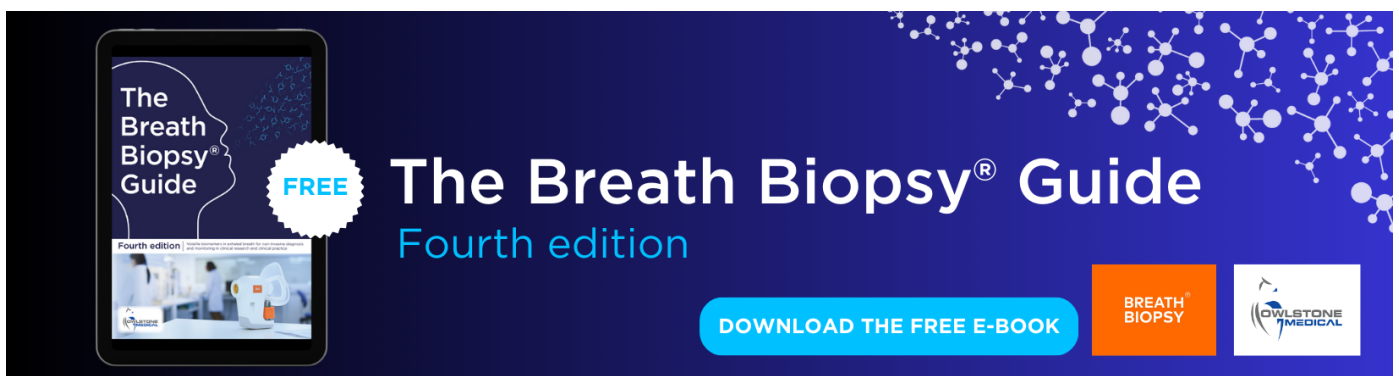
## Impacts of abiotic and biotic factors on tundra productivity near Utqiagvik, Alaska

To cite this article: Qingyuan Zhang *et al* 2023 *Environ. Res. Lett.* **18** 094070

View the [article online](#) for updates and enhancements.

You may also like

- [Reindeer grazing increases summer albedo by reducing shrub abundance in Arctic tundra](#)  
Mariska te Beest, Judith Sitters, Cécile B Ménard et al.
- [Exclusion of brown lemmings reduces vascular plant cover and biomass in Arctic coastal tundra: resampling of a 50 + year herbivore exclosure experiment near Barrow, Alaska](#)  
D R Johnson, M J Lara, G R Shaver et al.
- [Shrub growth and expansion in the Arctic tundra: an assessment of controlling factors using an evidence-based approach](#)  
Andrew C Martin, Elizabeth S Jeffers, Gillian Petrokofsky et al.



The Breath Biopsy® Guide  
Fourth edition

FREE

DOWNLOAD THE FREE E-BOOK

BREATH BIOPSY

OWLSTONE MEDICAL

ENVIRONMENTAL RESEARCH  
LETTERS

## LETTER

Impacts of abiotic and biotic factors on tundra productivity near  
Utqiagvik, Alaska

## OPEN ACCESS

RECEIVED  
7 June 2023REVISED  
26 August 2023ACCEPTED FOR PUBLICATION  
8 September 2023PUBLISHED  
18 September 2023

Original content from  
this work may be used  
under the terms of the  
[Creative Commons  
Attribution 4.0 licence](#).

Any further distribution  
of this work must  
maintain attribution to  
the author(s) and the title  
of the work, journal  
citation and DOI.

Qingyuan Zhang<sup>1,2,\*</sup> , Xuesong Zhang<sup>3,\*</sup> , Mark J Lara<sup>4,5</sup> , Zhengpeng Li<sup>6</sup> ,  
Kaiguang Zhao<sup>8</sup> and Tongxi Hu<sup>9</sup><sup>1</sup> Cooperate Institute for Satellite Earth System Studies, Earth System Science Interdisciplinary Center, University of Maryland, College Park, MD 20740, United States of America<sup>2</sup> Center for Satellite Applications and Research, NESDIS, NOAA, College Park, MD 20740, United States of America<sup>3</sup> USDA-ARS Hydrology and Remote Sensing Laboratory, Beltsville, MD 20705, United States of America<sup>4</sup> Department of Plant Biology, University of Illinois, Urbana, IL 61801, United States of America<sup>5</sup> Department of Geography, University of Illinois, Urbana, IL 61801, United States of America<sup>6</sup> GAMA-1 Technologies, 7500 Greenway Center Drive, STE 400, Greenbelt, MD 20770, United States of America<sup>7</sup> Earth Systems Research Center, Institute for the Study of Earth, Oceans, and Space, University of New Hampshire, Durham, NH 03824, United States of America<sup>8</sup> School of Environment and Natural Resources, Ohio Agricultural Research and Development Center, The Ohio State University, Wooster, OH 44691, United States of America<sup>9</sup> Institute for Sustainability Energy and Environment, University of Illinois, Urbana, IL 61801, United States of America

\* Authors to whom any correspondence should be addressed.

E-mail: [qyz72@yahoo.com](mailto:qyz72@yahoo.com) and [xuesong.zhang@usda.gov](mailto:xuesong.zhang@usda.gov)**Keywords:** Arctic tundra, earlier snowmelt, warming, lemming herbivory, fAPAR<sub>chl</sub>, productivitySupplementary material for this article is available [online](#)**Abstract**

Earlier snowmelt, warmer temperatures and herbivory are among the factors that influence high-latitude tundra productivity near the town of Utqiagvik in northern Alaska. However, our understanding of the potential interactions between these factors is limited. MODIS observations provide cover fractions of vegetation, snow, standing water, and soil, and fractional absorption of photosynthetically active radiation by canopy chlorophyll (fAPAR<sub>chl</sub>) per pixel. Here, we evaluated a recent time-period (2001–2014) that the tundra experienced large interannual variability in vegetation productivity metrics (i.e. fAPAR<sub>chl</sub> and APAR<sub>chl</sub>), which was explainable by both abiotic and biotic factors. We found earlier snowmelt to increase soil and vegetation cover, and productivity in June, while warmer temperatures significantly increased monthly productivity. However, abiotic factors failed to explain stark decreases in productivity during August of 2008, which coincided with a severe lemming outbreak. MODIS observations found this tundra ecosystem to completely recover two years later, resulting in elevated productivity. This study highlights the potential roles of both climate and herbivory in modulating the interannual variability of remotely retrieved plant productivity metrics in Arctic coastal tundra ecosystems.

**1. Introduction**

Monitoring, quantifying, and understanding changes in vegetation, snow cover and permafrost thaw in high latitude regions is fundamental for predicting how these regions and their inhabitants are impacted by climate change and how humans will need to adapt (Hinzman *et al* 2005, Carroll *et al* 2011, Arp *et al* 2013, Vincent *et al* 2013). Warming of northern latitudes has coincided with shifts in tundra vegetation (Mekonnen *et al* 2021), disappearing ponds and lakes

(Andresen and Lougheed 2015, Jones *et al* 2020), earlier snowmelt, lengthening of the growing season and start of spring greening and increase in tundra productivity (Myneni *et al* 1997, Wu *et al* 2022, Liu *et al* 2023).

High-latitude ecosystems are characterized by a short growing season and a long snow season (Serreze 2010, Zhang 2021). Warming and changes in the physio-hydrological environment has not only altered the timing of snowmelt and increased permafrost active layer thickness, but also plant production.

Table 1. Acronyms used in this study.

Acronym	Definition & Meaning
MODIS	The moderate resolution imaging spectrometer
AVHRR	The advanced very high resolution radiometer
PAR	Photosynthetically active radiation
APAR	Absorbed PAR
fAPAR	fractional absorption of PAR
fAPAR <sub>chl</sub>	fractional absorption of PAR by canopy chlorophyll
fAPAR <sub>non-chl</sub>	fractional absorption of PAR by canopy non-chlorophyll components
fAPAR <sub>canopy</sub>	fractional absorption of PAR by the entire canopy
APAR <sub>chl</sub>	Absorbed PAR by canopy chlorophyll (APAR <sub>chl</sub> = PAR × fAPAR <sub>chl</sub> )
LVS3	The coupled leaf-vegetation-soil-snow-surface water physical model
VGCF	Vegetation cover fraction per pixel
SOILCF	Soil cover fraction per pixel
SNOWCF	Snow cover fraction per pixel
WaterBodyCF	Standing water cover fraction per pixel
NDVI	Normalized difference vegetation index
GPP	gross primary productivity
SWI	Summer warmth index, i.e. the sum of average monthly temperature greater than 0 °C

The normalized difference vegetation index (NDVI) products from the advanced very high-resolution radiometer (AVHRR) have been often used to assess high latitude greening/browning trends. These studies used NDVI as a proxy of tundra productivity, and found pan-Arctic trends in NDVI to increase with the summer warmth index (SWI; the sum of average monthly temperature greater than 0 °C; Bhatt *et al* 2010). In addition to AVHRR datasets, satellite products from the moderate resolution imaging spectrometer (MODIS) and Landsat archives have been widely used with field observations to study Arctic vegetation dynamics (e.g. Stow *et al* 2004, Olofsson *et al* 2012, Epstein *et al* 2017, Berner *et al* 2020, Kim *et al* 2021). Many of these remotely sensed observations have led to new understanding of spatially and temporally dynamic ecological interactions. For example, Zona *et al* (2022) reported that earlier snowmelt was associated with greater Arctic gross primary productivity (GPP) in June and July, but lower GPP in August. The timing of snow melt also influences thermal properties that have impacts on thaw depth and local soil moisture and productivity (Jorgenson *et al* 2006, 2010, Jones *et al* 2011, Lara *et al* 2018a).

Though knowledge of the spatiotemporal linkages between abiotic factors and tundra productivity is growing, the short and long-term impacts of acute stochastic biotic disturbances is limited. In northern Alaska near the town of Utqiagvik, the impact of the dominant herbivore (i.e. brown lemming; *Lemmus trimucronatus*) on vegetation productivity was intensively studied during the early 1950s by field ecologists (Norton 2001). These early plot level experimental field studies reported that the digging of rhizomes by lemmings over the winter dramatically reduced the standing crop of forage by 20%–50% during the following summer (Thompson 1955, Schultz 1964). Field surveys during the recent 2008 lemming

population boom (Villarreal *et al* 2012) supported these early observations, dramatically reducing vegetation productivity metrics, GPP and NDVI (Lara *et al* 2017, Pitelka and Batzli 2007). Though short-term responses of defoliation directly reduced productivity, the long-term impacts of such intense biotic disturbances are more elusive and difficult to predict (Lara *et al* 2017). MODIS and AVHRR pixels in this region are often mixtures of soil, ponds, vegetation, and/or snow/melt. Soil, ponds, and snow/melt have confounding impacts on MODIS and AVHRR NDVI. In addition, NDVI has limited capability to distinguish between photosynthetic vegetation and non-photosynthetic vegetation (Zhang *et al* 2020, 2021).

Understanding the complex interactions between abiotic and biotic factors within data-rich subregions of the Arctic may improve our ability to interpret decadal-scale patterns and trends in remotely retrieved productivity metrics spanning tundra landscapes. Here, we evaluate the seasonal to decadal-scale variability in MODIS derived productivity metrics between 2001 to 2014, during a period of extraordinarily high variability in climate and environmental conditions (i.e. air temperature, downwelling and upwelling irradiance, and snowmelt date) and within the last known lemming population outbreak near Utqiagvik (i.e. 2008). The productivity metrics used in this study include the fractional absorption of photosynthetically active radiation (PAR) by canopy chlorophyll (fAPAR<sub>chl</sub>) and the absorption of PAR (APAR) by canopy chlorophyll (APAR<sub>chl</sub>) (Zhang 2021; table 1). The fAPAR<sub>chl</sub> is superior to NDVI in GPP estimation (Zhang *et al* 2005). Specifically, we address the following questions: (1) how did earlier snowmelt and air temperature affect the Utqiagvik (formerly Barrow) tundra productivity and surface cover fractions? and (2) how did the 2008 lemming outbreak impact remotely retrieved vegetation

productivity (e.g.  $fAPAR_{chl}$  and  $APAR_{chl}$ )? This study advances our ability to interpret spatial and temporal patterns and trends in remotely retrieved tundra productivity metrics.

## 2. Methods

### 2.1. Meteorological measurements

Our study examined the terrestrial land surface area of a  $7 \times 7$  km<sup>2</sup> region surrounding the US-Brw site (71.32° N, 156.61° W) near the town of Utqiagvik on the northern Barrow Peninsula of Alaska. This region is dominated by thermokarst lakes and drained thaw lake basins, which are composed of polygonal ice-wedge tundra (Brown *et al* 1980, Lara *et al* 2015, 2018b) (figure 1). NOAA's Earth System Research Laboratory (ESRL) at Utqiagvik measures downwelling and upwelling irradiance, wind, precipitation, and air temperature (Longenecker 2017, Vasel 2019). From 2001 to 2014, this area had a mean precipitation of 44.5 mm as rain during a three-month period from July through September. Mean annual temperature was  $-10.4$  °C, with lowest temperature in February ( $-24.6$  °C) and highest temperature in August ( $+4.2$  °C). The snow season spans from October to mid-May of the next year. Melting of snow increases soil moisture due to continuous permafrost and the low topographic relief (Hobbie 1984, Jepsen *et al* 2013, Carroll and Loboda 2017, Nitze *et al* 2017).

Upwelling irradiance increases with downwelling irradiance due to the presence of snow during the winter and early spring, then declines quickly with snowmelt. We utilized the method developed by Stone *et al* (2002) and the NOAA ESRL measurements of downwelling and upwelling irradiance to determine the snowmelt date: the first day of year (DOY) when the albedo started to be less than 0.3. The NOAA ESRL measurements of air temperature were used to compute SWI (Jia *et al* 2003; table 1).

We leveraged site-level observations near Utqiagvik to identify the timing of high lemming population densities (Johnson *et al* 2011, Villarreal *et al* 2012, Lara *et al* 2017). Lara *et al* (2017) reviewed the literature to chronologically record all known lemming outbreaks at our site, which occurred in 1946, 1949, 1953, 1956, 1960, 1965, 1971, 1976, 1981, 1986, 1991, 1996, 2000, 2003, and 2008. Due to the logistical challenges of continuous trapping needed to estimate annual lemmings ha<sup>-1</sup> in remote tundra regions, the long history of outbreak years remains among the most reliable and longest running boom-bust observations in the Arctic. We leverage these ground-based observations to advance our ability to remotely detect lemming outbreaks from space.

### 2.2. Satellite observations

At high latitudes, there are frequent MODIS overpasses that increase opportunities for clear sky data collections. MODIS data of land bands 1–7 at a 500 m

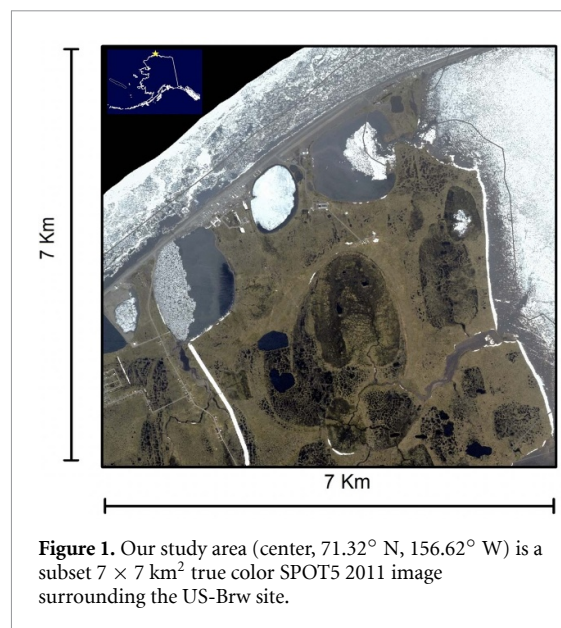


**Figure 1.** Our study area (center, 71.32° N, 156.62° W) is a subset  $7 \times 7$  km<sup>2</sup> true color SPOT5 2011 image surrounding the US-Brw site.

resolution (Masuoka 2019) from 2001 to 2014 were employed for the study region: blue (459–479 nm), green (545–565 nm), red (620–670 nm), near infrared (NIR<sub>1</sub>: 841–875 nm; NIR<sub>2</sub>: 1230–1250 nm), and shortwave infrared (SWIR<sub>1</sub>: 1628–1652 nm; SWIR<sub>2</sub>: 2105–2155 nm) (<https://ladsweb.modaps.eosdis.nasa.gov/archive/allData/6/MCD19A1>). We used high quality surface reflectance processed with the multi-angle implementation of atmospheric correction (MAIAC) algorithm (Lyapustin *et al* 2018). MAIAC is an advanced algorithm that uses time series analysis and a combination of pixel-based and image-based processing to improve accuracy of cloud/snow detection, aerosol retrievals, and atmospheric correction by incorporating the bidirectional reflectance distribution function model of the surface. The 500 m surface reflectance data were used to monitor the spatial and temporal dynamics of  $fAPAR_{chl}$  of the tundra ecosystem. The  $fAPAR_{chl}$  and fractional  $APAR$  by canopy non-chlorophyll components ( $fAPAR_{non-chl}$ ) were retrieved with surface reflectance of the seven bands and the coupled leaf-vegetation-soil-snow-standing water model (LVS3) (Zhang *et al* 2020, 2021).  $APAR_{chl}$  is the product of  $fAPAR_{chl}$  and  $PAR$  ( $APAR_{chl} = fAPAR_{chl} \times PAR$ ). In addition to the retrieval of the temporal dynamics of these productivity metrics, we also evaluated the coincident patterns in the cover fractions of vegetation (VGCF), soil (SOILCF), standing water (WaterBodyCF), and snow (SNOWCF) derived from MODIS (table 1). The Utqiagvik landscapes are often characterized by some portion of lakes, ponds, and seasonal freestanding water. The LVS3 model is a comprehensive model that depicts the interactions between leaf, vegetation, soil, snow, and surface water. It originated from the PROSAIL2 model (Zhang *et al* 2005, 2006, 2009, 2014a, 2014b, 2015, Cheng *et al* 2014). PROSAIL2 (PROSPECT + SAIL2) is a radiative

transfer model that simulates the reflection and transmission of solar radiation by vegetation and soil. The LVS3 model is a useful tool for studying the interactions between different land surface components, and for estimating various vegetation, water, snow and soil metrics using remote sensing data. Monthly VGCF, SOILCF, WaterBodyCF, SNOWCF,  $fAPAR_{chl}$  and  $fAPAR_{non-chl}$  products in April, May, June, July, August and September were produced from the MODIS observations with the LVS3 model. The chlorophyll molecules in vegetation absorb sunlight for energy to drive photosynthesis, which is a temperature-sensitive process (Raich *et al* 1991, Zhang *et al* 2005). Downwelling irradiance reached its peak in June.  $APAR_{chl}$  is computed with MODIS  $fAPAR_{chl}$  and the NOAA ESRL measurements-based PAR. 50% of shortwave radiation is in the PAR spectral interval (Pinker and Laszlo 1992, Frouin and Pinker 1995, Pinker *et al* 2010; [www2.atmos.umd.edu/~srb/par/webpar.htm](http://www2.atmos.umd.edu/~srb/par/webpar.htm)).

In addition to MODIS data, we acquired the Landsat TM images for this region during 2001–2014 at a 30 m resolution from Google Earth Engine (Hu *et al* 2021). July and August  $fAPAR_{chl}$  were retrieved. A summertime growth index was further derived as the  $fAPAR_{chl}$  difference between July and August. The deviation of the summertime growth in the year 2008 relative to the 14 years' average of the growth index was then computed as a measure to quantify fine-scale patterns of herbivory disturbances.

### 3. Results

#### 3.1. Utqiagvik meteorology

The 14 year average monthly PAR values from June to September were 130.47, 110.88, 62.69, and 28.78  $W m^{-2}$  respectively (figure 2(A)). The four average monthly PAR values were 39%, 33%, 19% and 9%, respectively, of the total PAR from June to September. The snow melt dates varied by 21 d, between DOY 145 (2002) and DOY 166 (2005, 2010) (figure 2(B)).

The 14 year monthly average temperature values from June to September were 0.03 °C, 3.62 °C, 4.50 °C, and 1.77 °C, respectively. Monthly temperatures in June, July, August and September showed increasing trends of 0.11 °C  $yr^{-1}$ , 0.10 °C  $yr^{-1}$ , 0.24 °C  $yr^{-1}$ , and 0.08 °C  $yr^{-1}$ , respectively, but only June values had a significant trend ( $F = 5.54$ ,  $p = 0.036 < 0.05$ ) (figure 2(C)). The 14 year SWI time series exhibited a significant increasing trend of 0.55 °C  $yr^{-1}$  ( $F = 6.81$ ,  $p = 0.023 < 0.05$ ; figure 2(D)).

#### 3.2. Cover fractions of vegetation, soil, water and snow

Evaluating interannual patterns of biophysical variables (e.g. vegetation, soil, surface water and snow

cover) provides insights into short and long-term patterns of ecological change (figure 3). The 2001–2014 average monthly PAR value declined from June to September. The 14 year average July and August temperature values were higher than the June and September values. Cover fractions of vegetation, soil, surface water and snow generally fluctuated from year to year, but we identified positive and negative trends in vegetation and soil cover fractions in July and August, respectively (figures 3(C) and (D)).

The 14 year decline in SOILCF for July and August was statistically significant (SOILCF for July:  $F = 4.84$ ,  $p = 0.0482 < 0.05$ ; SOILCF for August:  $F = 7.68$ ,  $p = 0.0208 < 0.05$ ). The annual percent changes of June, July, August and September VGCF were 0.46, 1.16, 0.66, and  $-1.58$ , respectively. The annual percent changes of June, July, August and September SOILCF were  $-1.46$ ,  $-1.28$ ,  $-2.42$ , and  $-2.14$ , respectively. The annual percent changes of June, July, August and September WaterBodyCF were 1.06,  $-0.58$ , 0.41, and 2.29, respectively.

#### 3.3. $fAPAR_{chl}$

Plant chlorophyll content is an important indicator of vegetation productivity in terrestrial ecosystems (Zhang *et al* 2005, 2014a). Typical Arctic tundra annual phenological patterns of  $fAPAR_{chl}$  begin with low values following snowmelt, steadily increase from June to August as vegetation growth expands spatially, and decline during the senescence period (figure 4(A)). The long-term average monthly  $fAPAR_{chl}$  values in June, July, August and September were 0.03, 0.16, 0.21 and 0.11, respectively. The annual percent changes of June, July, August and September  $fAPAR_{chl}$  were 0.55, 1.66, 0.98, and  $-1.70$ , respectively (figure 4(B)).

#### 3.4. $APAR_{chl}$

The importance of interannual changes in  $fAPAR_{chl}$  (figure 4(A)) to productivity was modulated by the strong seasonal variability in PAR (figure 2(A)). The 14 year averages for both  $fAPAR_{chl}$  and PAR in June and September differed greatly, with the  $fAPAR_{chl}$  value in September was about 4.2 times the  $fAPAR_{chl}$  value in June while the PAR value in June was about 4.5 times the PAR value in September. Therefore, the long-term averages for  $APAR_{chl}$  in June and September were similar (figure 4(A)).

The 14 year average monthly  $APAR_{chl}$  values in June, July, August and September were 110.30  $W m^{-2}$ , 567.82  $W m^{-2}$ , 429.96  $W m^{-2}$ , and 113.10  $W m^{-2}$ , respectively. Thus, percentages of monthly  $APAR_{chl}$  values to the entire growing season (June–September)  $APAR_{chl}$  value were 9%, 46.5%, 35.2% and 9.3%, respectively. Interannual variability in  $APAR_{chl}$  illustrates the effects of both chlorophyll content and cloudiness on productivity (figure 4(A)). The seasonal curve for  $APAR_{chl}$  differed from that of

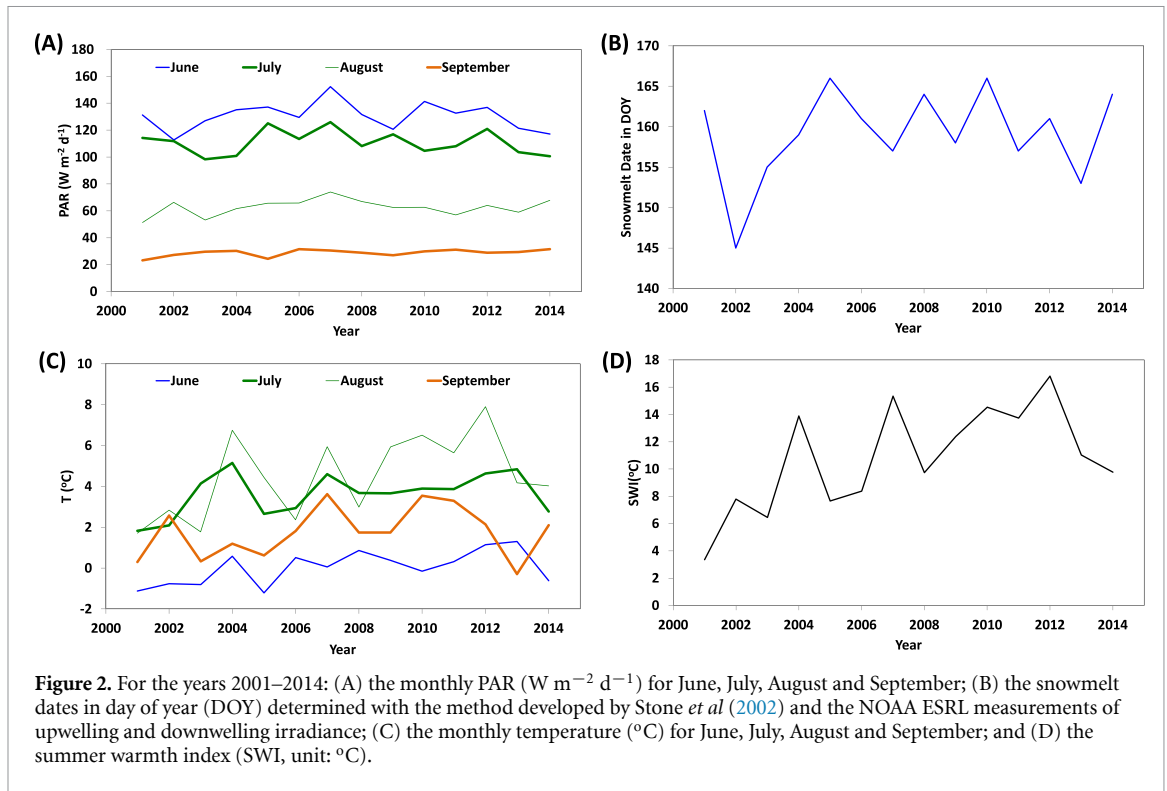


**Figure 2.** For the years 2001–2014: (A) the monthly PAR ( $W m^{-2} d^{-1}$ ) for June, July, August and September; (B) the snowmelt dates in day of year (DOY) determined with the method developed by Stone *et al* (2002) and the NOAA ESRL measurements of upwelling and downwelling irradiance; (C) the monthly temperature ( $^{\circ}C$ ) for June, July, August and September; and (D) the summer warmth index (SWI, unit:  $^{\circ}C$ ).

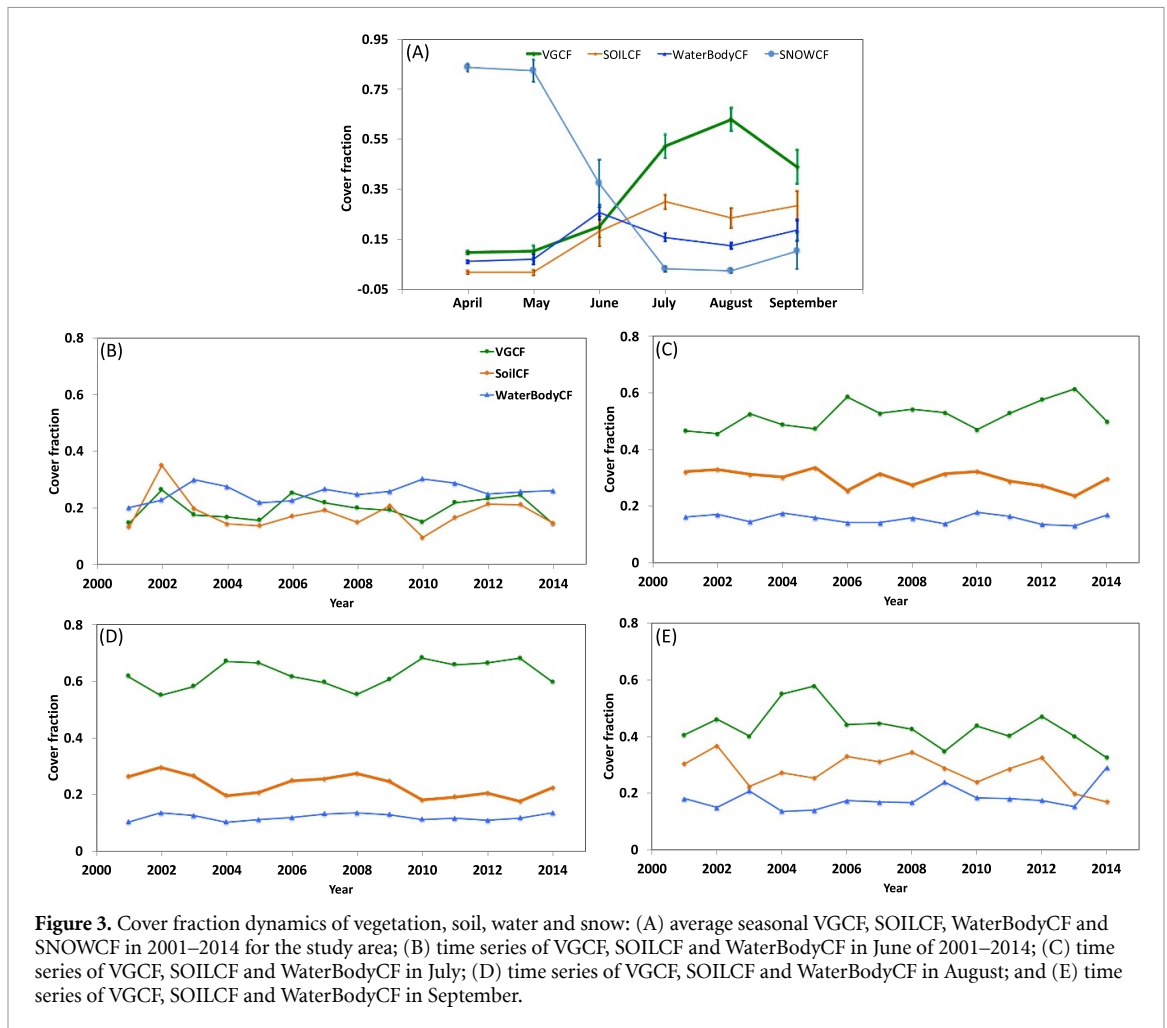


**Figure 3.** Cover fraction dynamics of vegetation, soil, water and snow: (A) average seasonal VGCF, SOILCF, WaterBodyCF and SNOWCF in 2001–2014 for the study area; (B) time series of VGCF, SOILCF and WaterBodyCF in June of 2001–2014; (C) time series of VGCF, SOILCF and WaterBodyCF in July; (D) time series of VGCF, SOILCF and WaterBodyCF in August; and (E) time series of VGCF, SOILCF and WaterBodyCF in September.

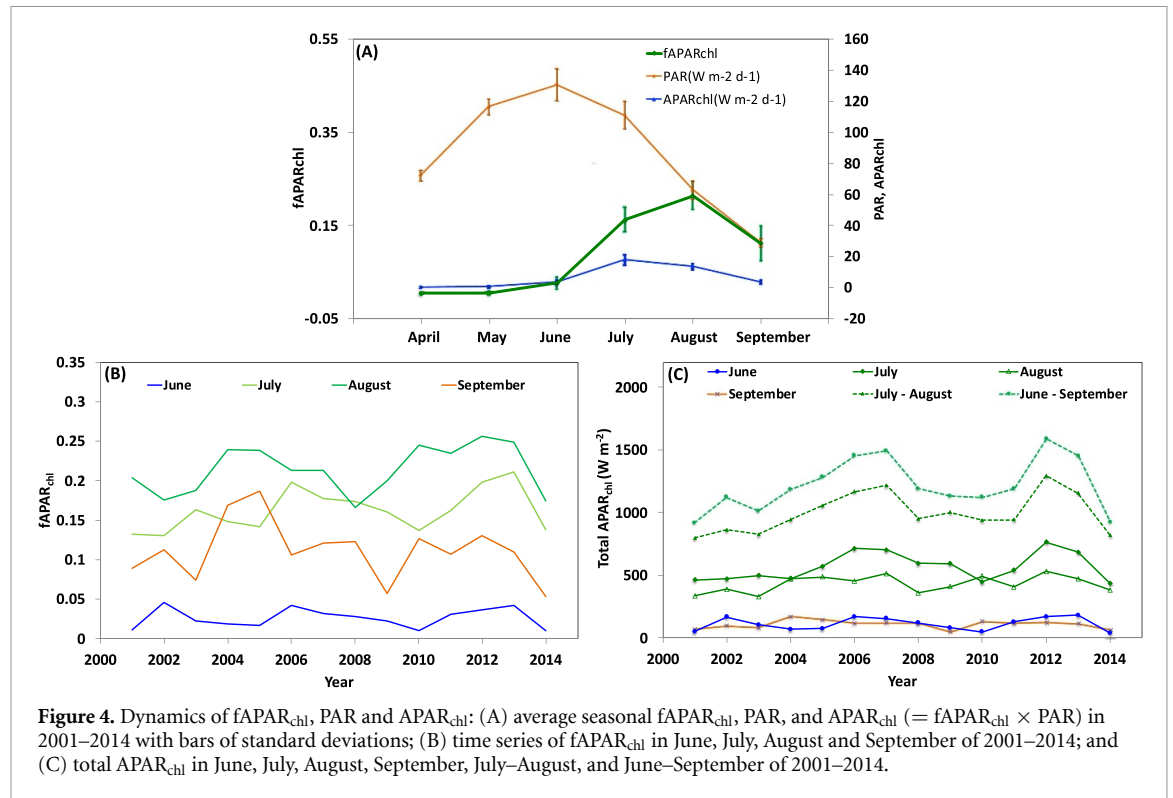


**Figure 4.** Dynamics of  $fAPAR_{chl}$ , PAR and  $APAR_{chl}$ : (A) average seasonal  $fAPAR_{chl}$ , PAR, and  $APAR_{chl}$  ( $= fAPAR_{chl} \times PAR$ ) in 2001–2014 with bars of standard deviations; (B) time series of  $fAPAR_{chl}$  in June, July, August and September of 2001–2014; and (C) total  $APAR_{chl}$  in June, July, August, September, July–August, and June–September of 2001–2014.

$fAPAR_{chl}$ , with the  $APAR_{chl}$  having sharper, higher, and earlier peak (figure 4(A)).

Since  $APAR_{chl}$  is closely related to productivity (Zhang *et al* 2014a), we show the multiyear variability in  $APAR_{chl}$  for June, July, August, September, July–August and the growing season (June–September) (figure 4(C)). There was large interannual variability in the growing season  $APAR_{chl}$ , which was mainly driven by variability in the  $APAR_{chl}$  for July–August. The large interannual variability previously shown for  $fAPAR_{chl}$  in September (figure 4(B)) was dampened for  $APAR_{chl}$  due to the low levels of incident PAR in September (figure 4(C)). The annual percent changes of June, July, August and September  $APAR_{chl}$  were 1.18, 1.46, 1.34, and  $-0.29$ , respectively. The annual percent change of July–August  $APAR_{chl}$  was 1.41. The annual percent change of June–September  $APAR_{chl}$  was 1.23 (figure 4(C)).

### 3.5. Influence of early snowmelt and temperature on vegetation

Relationships between the snowmelt date and (1) monthly  $fAPAR_{chl}$  in June, July, August, and September; (2) monthly  $APAR_{chl}$  in June, July, August and September; (3) total July–August  $APAR_{chl}$ ; and (4) total June–September  $APAR_{chl}$  were evaluated (figures 5(A) and (B)). The correlation between snowmelt date and monthly  $fAPAR_{chl}$  in June was significant (figure 5(A):  $F = 10.01$ ,  $p = 0.008 < 0.05$ ). The correlation between snowmelt date and monthly  $APAR_{chl}$  in June was significant (figure 5(B):  $F = 6.03$ ,  $p = 0.030 < 0.05$ ).

Relationships between the snowmelt date and monthly VGCF, SOILCF, SNOWCF and WaterBodyCF in June were evaluated (figure 5(C)). We observed a positive and significant correlation between snowmelt date and monthly VGCF and SOILCF in June (VGCF:  $F = 9.442$ ,  $p = 0.010 < 0.05$ ; SOILCF:  $F = 45.86$ ,  $p = 0.000 < 0.05$ ), but a negative and significant correlation between snowmelt date and monthly SNOWCF in June ( $F = 38.54$ ,  $p = 0.000 < 0.05$ ).

Temperature was an essential control of productivity on the Barrow Peninsula (Lara *et al* 2018a). SWI significantly impacted monthly  $fAPAR_{chl}$  for August (figure 6(A):  $F = 4.84$ ,  $p = 0.048 < 0.05$ ) and monthly  $APAR_{chl}$  for August ( $F = 13.03$ ,  $p = 0.004 < 0.05$ ) (figure 6(B)). SWI also had a significant impact on  $APAR_{chl}$  for July–August ( $F = 6.00$ ,  $p = 0.031 < 0.05$ ). As the contributions of  $APAR_{chl}$  in June and September to the growing season total  $APAR_{chl}$  were low, SWI had a significant impact on the growing season  $APAR_{chl}$  (June–September) ( $F = 5.30$ ,  $p = 0.040 < 0.05$ ).

Relationships of monthly temperature with monthly  $fAPAR_{chl}$  and  $APAR_{chl}$  were evaluated (figures 6(C) and (D)). Monthly temperature had a significant impact on monthly  $fAPAR_{chl}$  for July ( $F = 5.68$ ,  $p = 0.035 < 0.05$ ), and August ( $F = 8.77$ ,  $p = 0.012 < 0.05$ ). The effect of monthly temperature on monthly  $APAR_{chl}$  was significant for June ( $F = 4.76$ ,  $p = 0.0498 < 0.05$ ), and August ( $F = 15.58$ ,  $p = 0.002 < 0.05$ ).

Considering all monthly measurements from June to September in 2001–2014, we also observed

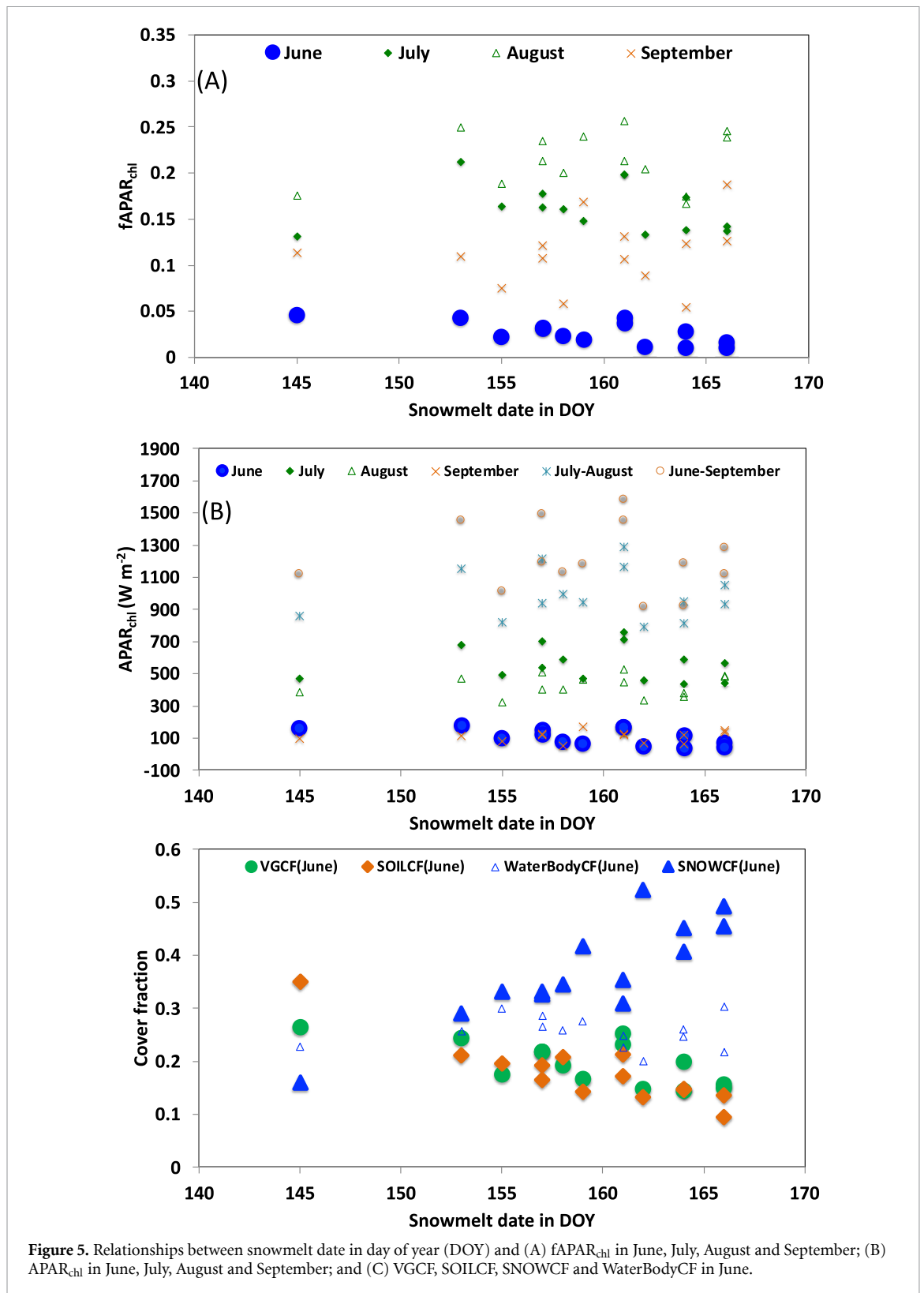


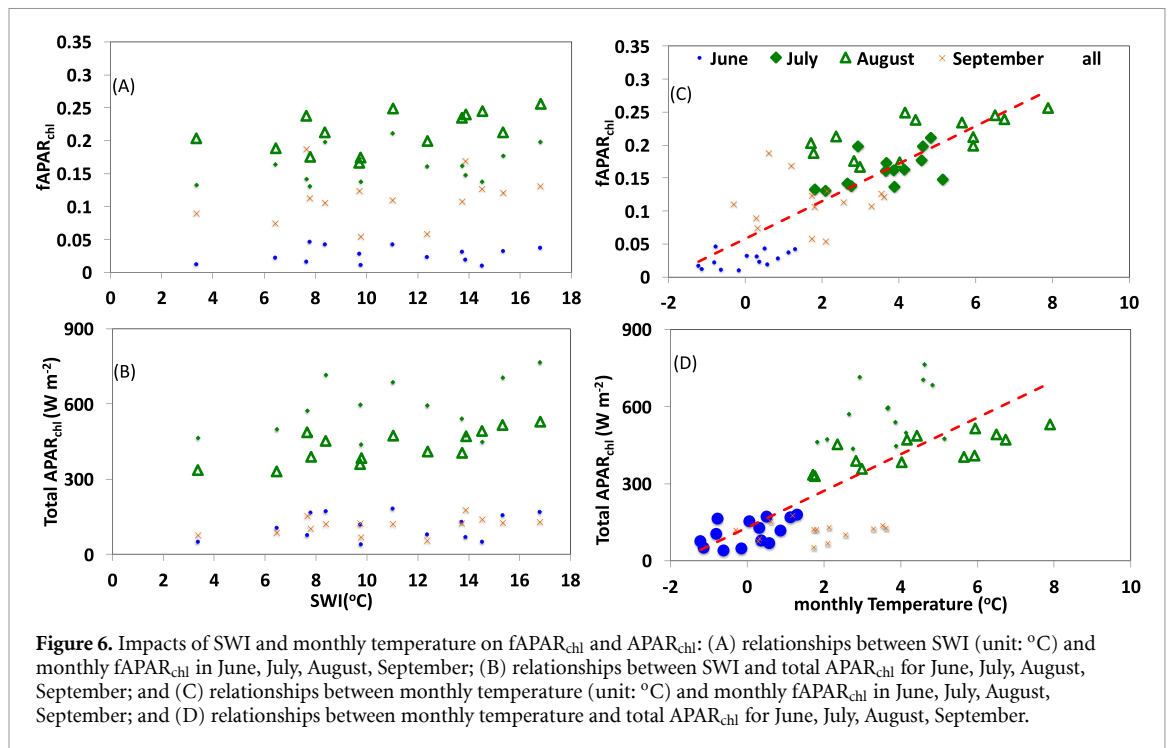
Figure 5. Relationships between snowmelt date in day of year (DOY) and (A)  $fAPAR_{chl}$  in June, July, August and September; (B)  $APAR_{chl}$  in June, July, August and September; and (C) VGCF, SOILCF, SNOWCF and WaterBodyCF in June.

that monthly temperature had a significant impact on monthly  $fAPAR_{chl}$  ( $F = 114.6, p = 0.000 < 0.05$ ), and  $APAR_{chl}$  ( $F = 61.07, p = 0.000 < 0.05$ ).

### 3.6. Influence of lemming herbivory on vegetation

Typically,  $fAPAR_{chl}$  increased from July to August as observed over the 14 year observation record (figure 4(A)). During the summer of 2008, a relatively

high lemming population outbreak caused severe vegetation defoliation (Johnson *et al* 2011, Villarreal *et al* 2012, Lara *et al* 2017).  $fAPAR_{chl}$  failed to increase from July to August in 2008 (figures 7(A) and (B)). Value of  $fAPAR_{chl}$  in July of 2008 was even greater than that in August due to the severe impact of the 2008 lemming population outbreak on foliage thus chlorophyll contents and  $fAPAR_{chl}$ . Figure 8 shows the



spatial pattern of the anomaly in summertime vegetation growth for the year 2008 relative to the average over 2001–2014.

Lemming herbivory resulted in consumption of live vegetation, decrease of standing dead, sharp drops in vegetation VGCF and  $fAPAR_{chl}$ , and an increase in bare ground (indicated by SOILCF) in 2008 (figure 7(C)). Results indicate the 2008 lemming outbreak year was also the only year with nearly identical VGCF and  $fAPAR_{chl}$  values for both July and August. The Utqiagvik tundra ecosystem mostly recovered in 2009, and completely recovered in 2010. Decadal and interannual patterns of  $fAPAR_{chl}$  were influenced not only by early snowmelt and temperature (figures 5 and 6) but also by the timing of intense arvicoline rodent herbivory.

#### 4. Discussion

Over a decade of MODIS observations near Utqiagvik finds that this tundra region experienced large interannual variability across all vegetation productivity metrics, driven by both abiotic and biotic factors. Due to the large interannual variability in all vegetation metrics in June, July and August, their trends were typically not within the 95% confidence level. Monthly  $fAPAR_{chl}$  and  $APAR_{chl}$  in June, July and August increased with temperature (figures 6(C) and (D)) and also increased over time (figures 4(B) and (C)), suggesting that warming may increase tundra greening and vegetation productivity. Furthermore, similar to Zona *et al* (2022), our results of  $fAPAR_{chl}$  and  $APAR_{chl}$  suggest that an earlier snowmelt may indicate an earlier green-up, and overall greater

vegetation productivity, specifically in June and July (figures 5(A) and (B)). These findings support the hypothesis that earlier snowmelt is indeed a predictor of higher Arctic production in June and July (Goetz *et al* 2005, Rosa *et al* 2015).

The NDVI from MODIS were computed and described in the supplementary material (figure S1). We found that an earlier snowmelt had a significant impact on monthly NDVI for June ( $F = 12.74$ ,  $p = 0.004 < 0.05$ ) (see figure S2(A)), not only due to the impact of earlier snowmelt on vegetation cover fraction (VGCF) for June ( $F = 9.44$ ,  $p = 0.010 < 0.05$ ) but also due to its impact on soil cover fraction (SOILCF) ( $F = 45.86$ ,  $p = 0.000 < 0.05$ ) (figure 5(C)). Seasonal VGCF,  $fAPAR_{chl}$  and  $APAR_{chl}$  profiles are different from seasonal NDVI profile (figures 3(A), 4(A) and S1(A)), hinting time series of VGCF,  $fAPAR_{chl}$  and  $APAR_{chl}$  may potentially provide alternative information for satellite-derived land surface phenology studies (Ye *et al* 2022, Zhang *et al* 2022), and for disturbance studies (Zhao *et al* 2018).

Although interannual controls on vegetation productivity are influenced by the timing of snowmelt, SWI and monthly temperature, our analysis finds local-scale dynamic disturbances confound decadal productivity trends. Due to the impact that lemmings can have on vegetation composition, nutrient cycling, and food web dynamics (Batzli *et al* 1980, Ims and Fuglei 2005), the severe lemming outbreak of 2008 was indeed noticeable from MODIS observations (figure 7). During the winter of 2007–2008, lemming likely grew rapidly under the snow and their population exploded during the summer of 2008 (Johnson *et al* 2011, Lara *et al* 2017). A high proportion of

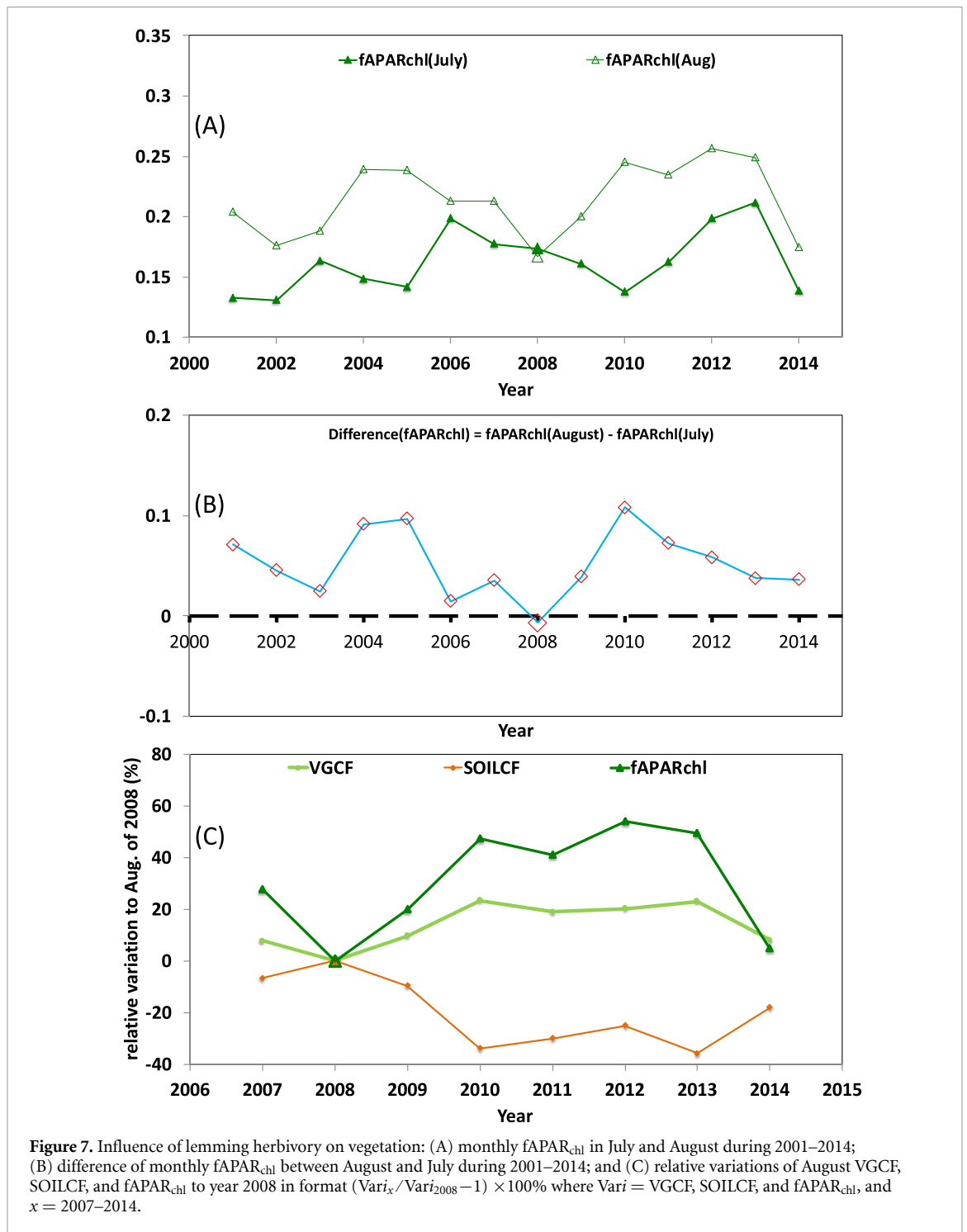
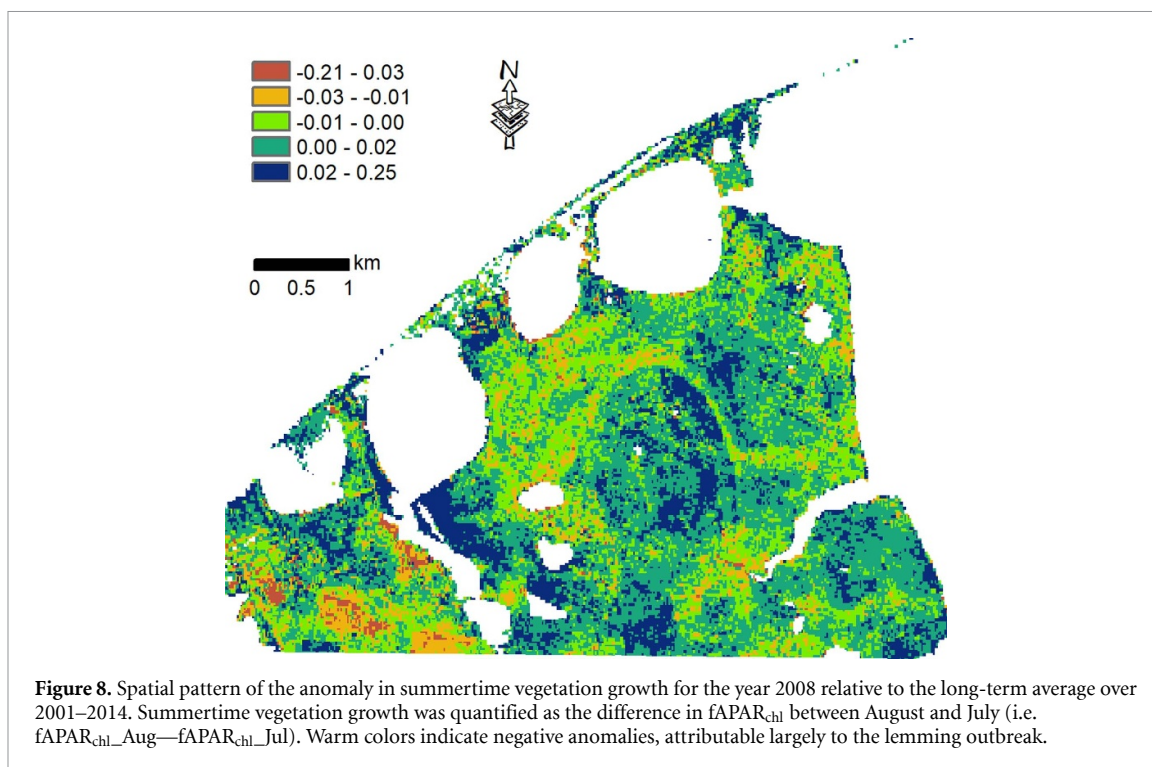


**Figure 7.** Influence of lemming herbivory on vegetation: (A) monthly fAPAR<sub>chl</sub> in July and August during 2001–2014; (B) difference of monthly fAPAR<sub>chl</sub> between August and July during 2001–2014; and (C) relative variations of August VGCF, SOILCF, and fAPAR<sub>chl</sub> to year 2008 in format  $(\text{Vari}_x / \text{Vari}_{2008} - 1) \times 100\%$  where Vari = VGCF, SOILCF, and fAPAR<sub>chl</sub>, and x = 2007–2014.

live vegetation was consumed during August of 2008, increasing bare ground and reducing standing dead across our study area (Johnson *et al* 2011, Villarreal *et al* 2012, Lara *et al* 2017). The MODIS observations support these field studies, as we also identified the lemming outbreak year to experience sharp declines in VGCF, fAPAR<sub>chl</sub>, and NDVI, and increase in SOILCF (figures 7(C) and S3(B)). Total PAR in June and July of 2014 was the lowest during 2001–2014, and the average temperature in June and July of 2014 was the lowest during 2006–2014. We observed a decrease in fAPAR<sub>chl</sub> during 2014 associated with

the climate anomaly (wet and cold), when lemming population densities were low (figures 2 and 7), highlighting the intricate interplay between abiotic and biotic factors that collectively control tundra vegetation productivity seasonally, interannually, and over decadal time-scales.

Following the lemming outbreak, MODIS observations show a gradual recovery in 2009, and a complete recovery by 2010, resulting in a ‘greener’ landscape with greater fAPAR<sub>chl</sub> than 2007 (figure 7(A)). This two-year vegetation recovery period (figure 7) is supported by field observations (Johnson *et al* 2011,



Villarreal *et al* 2012, Lara *et al* 2017) and predicted by the nutrient recovery hypotheses (Pitelka 1964, Batzli *et al* 1980, Pitelka and Batzli 2007). This hypothesis describes the process of rodent boom-bust dynamics, whereby high rodent population densities (i.e. boom) decimate the vegetation, increasing bare ground and altering surface energy balance (increasing thaw depth), which alters nutrient dynamics, resulting in reduced quality and quantity of forage. Lemming populations crash (i.e. bust) and gradually recover only when plant production increases, restoring surface energy balance and nutrient dynamics to levels that can meet the nutritional demands of high lemming population densities (Pitelka and Batzli 2007). However, perhaps most importantly, results find the lemming outbreak year to be the only year on record where monthly  $fAPAR_{chl}$  did not increase from July to August (figures 7(A) and (B)). The rare stability of monthly productivity metrics presents a new and exciting opportunity to use remote sensing to detect lemming outbreaks across vast regions of the Arctic. We will explore in this direction in the future.

## 5. Conclusions

We determined the importance of both abiotic and biotic factors in interpreting over a decade of trends, interannual variability and seasonal phenological patterns in vegetation productivity across the Barrow Peninsula. We found productivity metrics to increase with temperature and the SWI on decadal, interannual, and seasonal time scales, though earlier snowmelt consistently resulted in earlier green-up and overall greater annual vegetation

productivity. However, these traditionally important drivers/indicators can be shaken up during disturbance years, as highlighted during the 2008 lemming outbreak. In line with field observations, experiments, and the nutrient recovery hypothesis, we were able to characterize the vegetation recovery period with  $fAPAR_{chl}$  following disturbance. This satellite remote sensing analysis with LVS3 provided useful information for documenting surface changes in response to top-down and bottom-up driving factors, which may provide scientific support for understanding and managing high latitude ecosystems.

## Data availability statement

All data that support the findings of this study are included within the article (and any supplementary files).

## Acknowledgments

This work was partially funded by the NASA Terrestrial Ecology Program (Grant # NNX12AJ51G, PI: Q Zhang) and the Science of Terra and Aqua Program (Grant # NNX14AK50G, PI: Q Zhang). M J L is supported by NASA-ABOVE (80NSSC22K1254), NSF-EnvE (1928048), and DOE-TES (DE-SC0021094). Computational support and resources were provided by the NASA Center for Climate Simulation (NCCS) at Goddard Space Flight Center and the NASA High-End Computing (HEC) Program through the NASA Advanced Supercomputing (NAS) Division at Ames Research

Center. X Z is supported by the U.S. Department of Agriculture—Agricultural Research Service.

## ORCID iDs

Qingyuan Zhang  <https://orcid.org/0000-0003-0823-308X>

Mark J Lara  <https://orcid.org/0000-0002-4670-7031>

Jingfeng Xiao  <https://orcid.org/0000-0002-0622-6903>

## References

- Andresen C G and Lougheed V L 2015 Disappearing Arctic tundra ponds: fine-scale analysis of surface hydrology in drained thaw lake basins over a 65-year period (1948–2013) *J. Geophys. Res.* **120** 466–79
- Arp C D, Jones B M and Grosse G 2013 Recent lake ice-out phenology within and among lake districts of Alaska, U.S.A *Limnol. Oceanogr.* **58** 2013–28
- Batzli G O *et al* 1980 The herbivore-based tundra system *An Arctic Ecosystem: The Coastal Tundra at Barrow, Alaska* (Dowden, Hutchinson and Ross) pp 335–410
- Berner L T *et al* 2020 Summer warming explains widespread but not uniform greening in the Arctic tundra biome *Nat. Commun.* **11** 4621
- Bhatt U S *et al* 2010 Circumpolar Arctic tundra vegetation change is linked to sea ice decline *Earth Interact.* **14** 1–20
- Brown J *et al* 1980 *An Arctic Ecosystem: The Coastal Tundra at Barrow, Alaska* (Dowden, Hutchinson & Ross, Inc)
- Carroll M L *et al* 2011 Shrinking lakes of the Arctic: spatial relationships and trajectory of change *Geophys. Res. Lett.* **38** L20406
- Carroll M and Loboda T 2017 Multi-decadal surface water dynamics in North American Tundra *Remote Sens.* **9** 497–512
- Cheng Y-B, Zhang Q, Lyapustin A I, Wang Y and Middleton E M 2014 Impacts of light use efficiency and fPAR parameterization on gross primary production modeling *Agric. For. Meteorol.* **189–190** 187–97
- Epstein H *et al* 2017 Tundra Greenness (available at: [www.arctic.noaa.gov/Report-Card/Report-Card-2017/ArticleID/695/Tundra-Greenness](http://www.arctic.noaa.gov/Report-Card/Report-Card-2017/ArticleID/695/Tundra-Greenness))
- Frouin R and Pinker R T 1995 Estimating photosynthetically active radiation (PAR) at the earth's surface from satellite observations *Remote Sens. Environ.* **51** 98–107
- Goetz S J, Bunn A G, Fiske G J and Houghton R A 2005 Satellite-observed photosynthetic trends across boreal North America associated with climate and fire disturbance *Proc. Natl Acad. Sci.* **102** 13521–5
- Hinzman L D *et al* 2005 Evidence and implications of recent climate change in Northern Alaska and other Arctic regions *Clim. Change* **72** 251–98
- Hobbie J E 1984 *The Ecology of Tundra Ponds of the Arctic Coastal Plain: A Community Profile* (Fish and Wildlife Service)
- Hu T, Myers Toman E, Chen G, Shao G, Zhou Y, Li Y, Zhao K and Feng Y 2021 Mapping fine-scale human disturbances in a working landscape with Landsat time series on Google Earth Engine *ISPRS J. Photogramm. Remote Sens.* **176** 250–61
- Ims R A and Fuglei E 2005 Trophic interaction cycles in tundra ecosystems and the impact of climate change *BioScience* **55** 311–22
- Jepsen S M, Voss C I, Walvoord M A, Minsley B J and Rover J 2013 Linkages between lake shrinkage/expansion and sublacustrine permafrost distribution determined from remote sensing of interior Alaska, USA *Geophys. Res. Lett.* **40** 882–7
- Jia G J, Epstein H E and Walker D A 2003 Greening of arctic Alaska 1981–2001 *Geophys. Res. Lett.* **30** GL018268
- Johnson D R, Lara M J, Shaver G R, Batzli G O, Shaw J D and Tweedie C E 2011 Exclusion of brown lemmings reduces vascular plant cover and biomass in Arctic coastal tundra: resampling of a 50+ year herbivore enclosure experiment near Barrow, Alaska *Environ. Res. Lett.* **6** 045507
- Jones B M *et al* 2020 Identifying historical and future potential lake drainage events on the western Arctic coastal plain of Alaska *Permafrost. Periglac. Process.* **31** 110–27
- Jones B M, Grosse G, Arp C D, Jones M C, Walter Anthony K M and Romanovsky V E 2011 Modern thermokarst lake dynamics in the continuous permafrost zone, northern Seward Peninsula, Alaska *J. Geophys. Res.* **116** G00M03
- Jorgenson M T, Romanovsky V, Harden J, Shur Y, O'Donnell J, Schuur E A G, Kanevskiy M and Marchenko S 2010 Resilience and vulnerability of permafrost to climate change *Can. J. For. Res.* **40** 1219–36
- Jorgenson M T, Shur Y L and Pullman E R 2006 Abrupt increase in permafrost degradation in Arctic Alaska *Geophys. Res. Lett.* **33** L02503
- Kim J, Kim Y, Zona D, Oechel W, Park S-J, Lee B-Y, Yi Y, Erb A and Schaaf C L 2021 Carbon response of tundra ecosystems to advancing greenup and snowmelt in Alaska *Nat. Commun.* **12** 6879
- Lara M J, Johnson D R, Andresen C, Hollister R D and Tweedie C E 2017 Peak season carbon exchange shifts from a sink to a source following 50+ years of herbivore exclusion in an Arctic tundra ecosystem *J. Ecol.* **105** 122–31
- Lara M J, McGuire A D, Euskirchen E S, Tweedie C E, Hinkel K M, Skurikhin A N, Romanovsky V E, Grosse G, Bolton W R and Genet H 2015 Polygonal tundra geomorphological change in response to warming alters future CO<sub>2</sub> and CH<sub>4</sub> flux on the Barrow Peninsula *Glob. Change Biol.* **21** 1634–51
- Lara M J, Nitze I, Grosse G, Martin P and McGuire A D 2018a Reduced arctic tundra productivity linked with landform and climate change interactions *Sci. Rep.* **8** 1–10
- Lara M J, Nitze I, Grosse G and McGuire A D 2018b Tundra landform and vegetation productivity trend maps for the Arctic coastal plain of northern Alaska *Sci. Data* **5** 1–10
- Liu Y, Wu C, Wang X and Zhang Y 2023 Contrasting responses of peak vegetation growth to asymmetric warming: evidences from FLUXNET and satellite observations *Glob. Change Biol.* **29** 2363–79
- Longenecker D 2017 NOAA/ESRL/GMD/GRAD (available at: <http://aftp.cmdl.noaa.gov/data/radiation/baseline/brw/>)
- Lyapustin A, Wang Y, Korkin S and Huang D 2018 MODIS Collection 6 MAIAC Algorithm *Atmos. Meas. Tech.* **11** 5741–65
- Masuoka E 2019 Search and order from LAADS (available at: <https://ladsweb.nascom.nasa.gov:9400/data/>)
- Mekonnen Z A *et al* 2021 Arctic tundra shrubification: a review of mechanisms and impacts on ecosystem carbon balance *Environ. Res. Lett.* **16** 053001
- Myneni R B, Keeling C D, Tucker C J, Asrar G and Nemani R R 1997 Increased plant growth in the northern high latitudes from 1981 to 1991 *Nature* **386** 698–702
- Nitze I, Grosse G, Jones B, Arp C, Ulrich M, Fedorov A and Veremeeva A 2017 Landsat-based trend analysis of lake dynamics across northern permafrost regions *Remote Sens.* **9** 640
- Norton D W 2001 *Fifty More Years Below Zero* (Arctic Institute of North America)
- Olofsson J, Tommervik H and Callaghan T V 2012 Vole and lemming activity observed from space *Nat. Clim. Change* **2** 880–3
- Pinker R T and Laszlo I 1992 Global distribution of photosynthetically active radiation as observed from satellites *J. Clim.* **5** 56–65
- Pinker R T, Zhao M, Wang H and Wood E F 2010 Impact of satellite based PAR on estimates of terrestrial net primary productivity *Int. J. Remote Sens.* **31** 5221–37

- Pitelka F A and Batzli G O 2007 Population cycles of lemmings near Barrow, Alaska: a historical review *Acta Theriol.* **52** 323–36
- Pitelka F A 1964 The nutrient-recovery hypothesis for arctic microtine cycles. I. Introduction *Grazing in Terrestrial and Marine Environments* ed D J Crisp (Blackwell, British Ecological Society Symposium) pp 55–56
- Raich J W, Rastetter E B, Melillo J M, Kicklighter D W, Steudler P A, Peterson B J, Grace A L, Moore B and Vorosmarty C J 1991 Potential net primary productivity in South-America—application of a global-model *Ecol. Appl.* **1** 399–429
- Rosa R K, Oberbauer S F, Starr G, Parker La Puma I, Pop E, Ahlquist L and Baldwin T 2015 Plant phenological responses to a long-term experimental extension of growing season and soil warming in the tussock tundra of Alaska *Glob. Change Biol.* **21** 4520–32
- Schultz A M 1964 The nutrient-recovery hypothesis for arctic microtine cycles II. Ecosystem variables in relation to the arctic microtine cycles. *A Symp. British Ecological Society (Bangor, 11–14 April 1962)* ed D J Crisp (Blackwell) pp 57–68
- Serreze M C 2010 Understanding recent climate change *Conserv. Biol.* **24** 10–17
- Stone R, Dutton E G, Harris J M and Longenecker D 2002 Earlier spring snowmelt in northern Alaska as an indicator of climate change *J. Geophys. Res.* **107** 4089
- Stow D A et al 2004 Remote sensing of vegetation and land-cover change in Arctic Tundra Ecosystems *Remote Sens. Environ.* **89** 281–308
- Thompson D Q 1955 The 1953 lemming emigration at Point Barrow, Alaska *Arctic* **8** 37–45
- Vasel B 2019 Meteorology Measurements from the NOAA/ESRL/GMD Baseline Observatories (available at: <ftp://aftp.cmdl.noaa.gov/data/meteorology/in-situ/brw/>)
- Villarreal S, Hollister R D, Johnson D R, Lara M J, Webber P J and Tweedie C E 2012 Tundra vegetation change near Barrow, Alaska (1972–2010) *Environ. Res. Lett.* **7** 015508
- Vincent W F et al 2013 Climate impacts on Arctic lake ecosystems *Climatic Change and Global Warming of Inland Waters: Impacts and Mitigation for Ecosystems and Societies* ed C R Goldman, M Kumagai and R D Robarts (Wiley)
- Wu C et al 2022 Increased drought effects on the phenology of autumn leaf senescence *Nat. Clim. Change* **12** 943–9
- Ye Y, Zhang X, Shen Y, Wang J, Crimmins T and Scheffinger H 2022 An optimal method for validating satellite-derived land surface phenology using in-situ observations from national phenology networks *ISPRS J. Photogramm. Remote Sens.* **194** 74–90
- Zhang Q et al 2006 Characterization of seasonal variation of forest canopy in a temperate deciduous broadleaf forest, using daily MODIS data *Remote Sens. Environ.* **105** 189–203
- Zhang Q 2021 Characterization of a seasonally snow-covered evergreen forest ecosystem *Int. J. Appl. Earth Obs. Geoinf.* **103** 102464
- Zhang Q, Cheng Y-B, Lyapustin A I, Wang Y, Gao F, Suyker A, Verma S and Middleton E M 2014a Estimation of crop gross primary production (GPP): fAPARchl versus MOD15A2 FPAR *Remote Sens. Environ.* **153** 1–6
- Zhang Q, Cheng Y-B, Lyapustin A I, Wang Y, Xiao X, Suyker A, Verma S, Tan B and Middleton E M 2014b Estimation of crop gross primary production (GPP): I. Impact of MODIS observation footprint area and impact of vegetation BRDF characteristics *Agric. For. Meteorol.* **191** 51–63
- Zhang Q, Cheng Y-B, Lyapustin A I, Wang Y, Zhang X, Suyker A, Verma S, Shuai Y and Middleton E M 2015 Estimation of crop gross primary production (GPP): II. Do the scaled vegetation indices improve performance? *Agric. For. Meteorol.* **200** 1–8
- Zhang Q, Middleton E M, Margolis H A, Drolet G G, Barr A A and Black T A 2009 Can a MODIS-derived estimate of the fraction of PAR absorbed by chlorophyll (FAPAR<sub>chl</sub>) improve predictions of light-use efficiency and ecosystem photosynthesis for a boreal aspen forest? *Remote Sens. Environ.* **113** 880–8
- Zhang Q, Xiao X, Braswell B, Linder E, Baret F and Moore B 2005 Estimating light absorption by chlorophyll, leaf and canopy in a deciduous broadleaf forest using MODIS data and a radiative transfer model *Remote Sens. Environ.* **99** 357–71
- Zhang Q, Yao T, Huemmrich K F, Middleton E M, Lyapustin A and Wang Y 2020 Evaluating impacts of snow, surface water, soil and vegetation on empirical vegetation and snow indices for the Utqiagvik tundra ecosystem in Alaska with the LVS3 model *Remote Sens. Environ.* **240** 111677
- Zhang X, Shen Y, Gao S, Wang W and Schaaf C 2022 Diverse responses of multiple satellite-derived vegetation greenup onsets to dry periods in the Amazon *Geophys. Res. Lett.* **49** e2022GL098662
- Zhao F et al 2018 Development of Landsat-based annual US forest disturbance history maps (1986–2010) in support of the North American Carbon Program (NACP) *Remote Sens. Environ.* **209** 312–26
- Zona D et al 2022 Earlier snowmelt may lead to late season declines in plant productivity and carbon sequestration in Arctic tundra ecosystems *Sci. Rep.* **12** 3986